



Numerical and Experimental Comparison of Passive Cooling Effect on Photovoltaic- Thermoelectric Generator hybrid System Performance

Ali Ajib SALBOOKH¹, Mohammed Wahhab ALJİBORY² & Hasan Talib HASHİM³

Keywords

Hybrid system, thermoelectric generator, passive cooling, harvesting, solar energy, numerical simulation.

Abstract

In this paper, a 3D numerical model to investigate the efficiency of solar energy harvesting using photovoltaic panels combined with thermoelectric generator modules (PV-TEG) was built. Furthermore, the effects of different numbers and distributions of thermoelectric modules by using a passive cooling unit on the performance of PV-TEG system were investigated. Seven models of hybrid system (M1-M7) with different numbers and distributions of TEG items were tested and simulated numerically. In addition, the optimum model performance of (PV-TEG) was compared with that of photovoltaic only and photovoltaic/thermal (PV/T) system. Based on the results obtained, the optimum model of hybrid system was M1. Also, electrical power of the PV-TE system, when exposed to solar radiation of 1000 W/m² and ambient temperature of 25 °C, was higher by 16.3% and 1.79% than that of the PV only and PV/T system, respectively. Besides, performance of M1 model was validated by experimental work in the indoor environment under the same operation conditions. The experimental results showed that the enhancement ratio of P_{el} of the (M1) model is higher by 15.13 and 0.8 % compared with the photovoltaic panel and the PV/T system. It can be seen that the numerical results for all studied parameters show a good level of agreement with experimental results. Ultimately, the effect of passive cooling on the PV-TEG system performance was lower.

Article History

Received
11 Mar, 2023
Accepted
23 Jun, 2023

1. Introduction

Solar energy is unity of best ways to chance the world's energy needs besides fossil fuels because it lasts longer, costs less, and is easy to get. Even though thermal and photovoltaic (PV) technologies are used, PV systems are more popular because they can change energy directly. Only 15–20% of the solar irradiance is converted to electricity due to the PV module's sensitivity to the visible light spectrum; the rest is dissipated as heat (Mahmoudinezhad et al. 2018). The module's efficiency

¹ Corresponding Author. ORCID: 0000-0003-3557-4488. Mechanical Engineering Department, College of Engineering, Kerbala University, Karbala, Iraq, ali.ajib@s.uokerbala.edu.iq

² ORCID: 0000-0001-7817-0673. Mechanical Engineering Department, College of Engineering, Kerbala University, Karbala, Iraq, Dr.mohammad.wahab@s.uokerbala.edu.iq

³ ORCID: 0000-0001-6771-5543. Biomedical Engineering Department, College of Engineering, Kerbala University, Karbala, Iraq, hasanth2025@s.uokerbala.edu.iq

drops by 0.45% per degree Celsius as the working temperature rises (M W Aljibory 2021). The sweet spot is between 25 and 35 degrees Celsius (Han Xue, Zhao Guankun, Xu Chao, Ju Xing, Du Xiaoze and Key 2017).

Nomenclature			
A_{pv}	Solar panel surface area, m^2	ρ	Electrical resistance, $\mu\Omega \cdot m$
G	Solar irradiance, $W m^{-2}$	τ	Transmissivity
Subscripts			
E	Power, W	amb	Ambient
k	Conductivity, $W m^{-1} K^{-1}$	el	Electrical
T	Temperature, K	o	Standard condition
Z	Figure of merit	g	Glass
Greek			
α	Absorptivity	TEG	Thermoelectric generator
μ	Viscosity, $kg m^{-1} s^{-1}$	w	Wind
η	Efficiency, %	$PV-TEG$	Photovoltaic-Thermoelectric hybrid system

In order to control module temperature, researchers have used optical therapy and/or thermal management. Optical treatment is effective, but the expense is debatable (Adham Makki, Siddig Omer, Yuehong Su 2016). Because of this, many people are researching thermal management techniques. Either active methods (such as fluid circulation using a pump or fan) or passive ways can be used to accomplish it (natural convection or wall conduction). The latter is energy-free and can cool the module by 6 to 20 degrees Celsius while the former uses additional energy to cool the module to a maximum of 30 degrees (Mohsenzadeh, Shafii, and Jafari mosleh 2017).

Therefore, fins, phase change materials (PCM), cotton wicks, heat pipes, liquid immersion, selective coating, besides other passive techniques are actively being researched (Krishnadass Karthick, Suresha, Mohammed Muaaz M.D. Hussain, Hafiz Muhammad Ali 2019), (Samson Shittu, Guiqiang Li, Yousef Golizadeh Akhlaghi, Xiaoli Ma, Xudong Zhao 2019), (Babu and Ponnambalam 2017), and (H. Hashim, J.J. Bompfrey 2016). Thermo-electric generators (TEG), the newest member of this group, are frequently referred to as hybrid cooling methods since they simultaneously create electric power and have a cooling impact on PV modules (Gu et al. 2019).

TEG modules are a semiconductor device that use the Seebeck effect to generate an electrical current from a temperature difference across a p-n junction. The key advantages of TE modules are their low environmental impact, ease of use, silence of operation, durability, and lack of moving components (Dianhong Li, Yimin Xuan, Qiang Li 2017) and (M. Hajji, H. Labrim, M. Benaissa, A. Laazizi, H. Ez-Zahraouy, E. Ntsoenzok, J. Meot 2017). However, its inefficiency is their primary downside. In contrast, as technology improves, their efficacy increases (Yin, Li, and Xuan 2017) and (Hashim 2015). Numerous researchers are examining viability of using thermoelectric generators in diverse applications, for instance waste heat recovery from automobiles (Riahia, Afifa, Abdessalem Ben Haj Ali, Abdelhamid Fadhel, Amenallah Guizani 2020), electrical ovens (Darkwaa, J., J. Calautit, D. Du 2019), fuel cells (Mohammad Sardarabadi 2016), net-zero energy buildings (NZEB) (Mohamed Selmi, Mohammed J. Al-Khawaja 2008), also building heating and cooling (Evans 1981).

Some researchers have started to investigate the possibility of combining TE modules with PV systems in addition to the previously listed applications of TE technology (Mahmoudinezhad et al. 2018) (M W Aljibory 2021) (Han Xue, Zhao Guankun, Xu Chao ↑, Ju Xing, Du Xiaoze and Key 2017) (Adham Makki, Siddig Omer, Yuehong Su 2016) (Mohsenzadeh et al. 2017), To maximize the use of solar energy, it is necessary to improve the efficiency with which it is converted.. Lately, (Krishnadass Karthick, Suresha, Mohammed Muaaz M.D. Hussain, Hafiz Muhammad Ali 2019) hybrid PV-TEG systems (without any beam splitter) for cogeneration purposes coupled with PCM have been evaluated and suggested. (Samson Shittu, Guiqiang Li, Yousef Golizadeh Akhlaghi, Xiaoli Ma, Xudong Zhao 2019) and (Babu and Ponnambalam 2017) the importance of passive cooling in TEG systems to lower operational costs, and the potential future of hybrid systems for cogeneration.

The majority of PV-TEG research is theoretical and/or computational. (H. Hashim, J.J. Bomphrey 2016) optimized geometry of a hybrid structure aimed at waste heat recovery using a numerical model created in MATLAB. We discussed the trade-off between power output and thermoelectric material demand, as the TEG module with the lower cross-sectional area (relative to the PV module) resulted in a bigger power than the big cross-sectional areas. (Gu et al. 2019) The thermal contact resistance was found to have a major influence in the overall performance of the hybrid system when simulated mathematically and numerically (using water for cooling and a glass tube as the concentrator. (Dianhong Li, Yimin Xuan, Qiang Li 2017) performed energy and exergy analysis of PV-TE hybrid power systems. This study used a 1D model to analyze the effects of varying concentration ratios and PV module technologies on the overall performance of a PV-TE system.

(M. Hajji, H. Labrim, M. Benaissa, A. Laazizi, H. Ez-Zahraouy, E. Ntsoenzok, J. Meot 2017) Numerical analysis was used to examine the efficiency of indirect coupling of PV and TE modules. Between the photovoltaic and thermoelectric modules, they placed a concentrator to maximize solar energy harvesting. They arrived at the inference that indirect coupling considerably improved the system's overall efficiency. Nonetheless, in particular, TEG parameters viz. p-n connection density, arm length, cross-sectional area, and distance are all relevant variables. Only a few numerical studies, including flat plate (PCM), and water, have focused on cooling strategies for TEG in PV-TEG systems Yin et al. (Yin et al. 2017).

Hence, objectives of the present numerical study are analysis of PV-TEG system performance in multi configuration models under the indoor environment by using a heat sink and incorporating natural convection of air (passive cooling). also, detecting the appropriated number and distribution of TEG modules that achieves high difference temperature and maximum output energy when integrating with PV panel. Furthermore, the performance the best model of hybrid system would be compared with that of PV panel only and PV/T system with passive cooling.

2. Methodology

2.1. System Description

The current research makes use of a 3D numerical model to examine the thermal and performance characteristics of PV panel, PV/T, and PV-TEG systems. The

model of the PV-TEG system is shown in Figure (1). The PVT system is identical to the PV-TEG system except that the TE module layer is omitted. The TEG modules are situated between the Tedlar layer and the heat sink to accommodate the high temperature difference between them. Toward transfer heat from the photovoltaic panels to thermoelectric generator(TEG) modules (hot side), an aluminum conductor plate is located to the top of the PV panels (Hashim 2015). As depict in Figure (2a), the created model takes into account all of the layers that make up a polycrystalline silicon PV module.

Furthermore, Figure (2b) displays a layering diagram of the TEG (TEC-12715) module. The TEG consists of the following layers ; ceramic, 127 pairs of n-type too p-type thermo elements composed of (Bi₂Te₃) semiconductor materials that supply the electrical connation in the TEG, and ceramic provides thermal conductivity (Mahmoudinezhad et al. 2018). The heat sink is aluminum base plate with fins as shown in Figure (2c)

The thermo physical characteristics of the emulator systems are offered in Table (1).

Figure 1. The simulated PV-TEG system

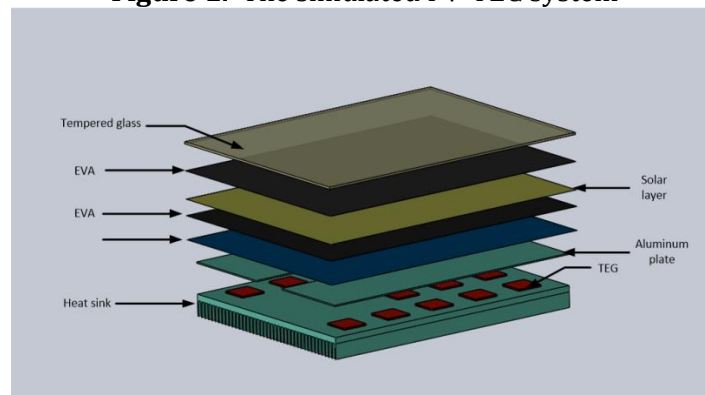
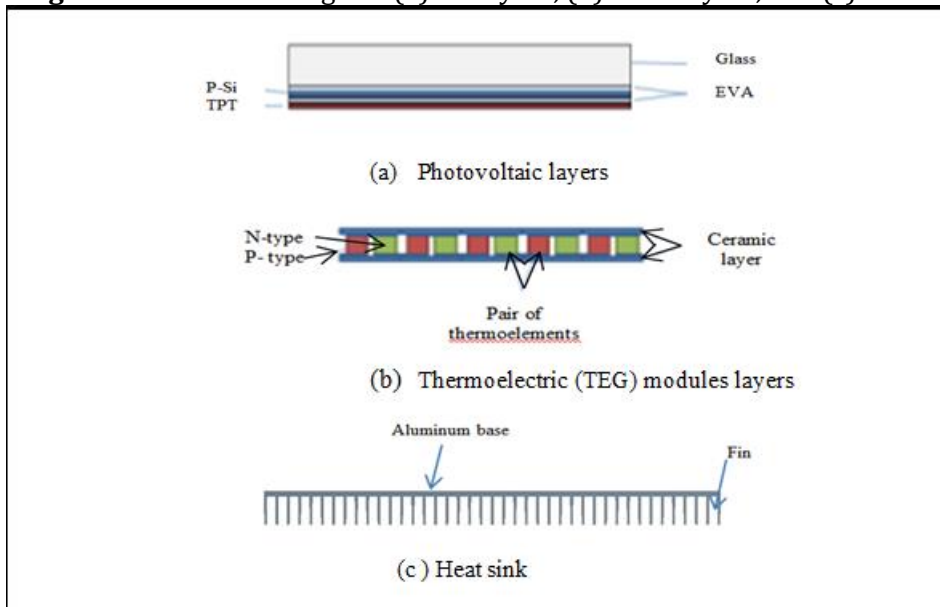


Table 1. Thermo physical characteristics of the PV-TEG systems (Riahia, Afifa, Abdessalem Ben Haj Ali, Abdelhamid Fadhel, Amenallah Guizani 2020) and (Darkwaa, J., J. Calautit, D. Du 2019)

Layer	Heat capacity, Cp [J/(kgK)]	Density, ρ [kg/m ³]	Thermal conductivity, k [W/(m.K)]	Dimensions(mm) (L x W x H)
Glass	500	2450	2	450x 340 x 3.2
EVA	2090	960	0.311	450x 340 x 0.4
Silicon	677	233	130	450x 340 x 0.18
EVA	2090	960	0.311	450x 340 x 0.4
TPT	1250	1200	0.15	450x 340 x 0.18
Air	1005	1.205	0.0271	-
Ceramic	880	3720	25	40 x 40 x 0.5
Bi ₂ Te ₃ (p-n types)	708.4	92.74	0.92	40 x 40 x 2
Aluminum	871	2719	202.4	
1. Plate				325 x 428 x 2
2. heat sink base				325 x 428 x 9.5
3. Fin (41 fin)				325 x 1.7 x 23.5

Figure 2. Schematic diagram (a) PV layers, (b) TEG- layers, and (c) Heat sink

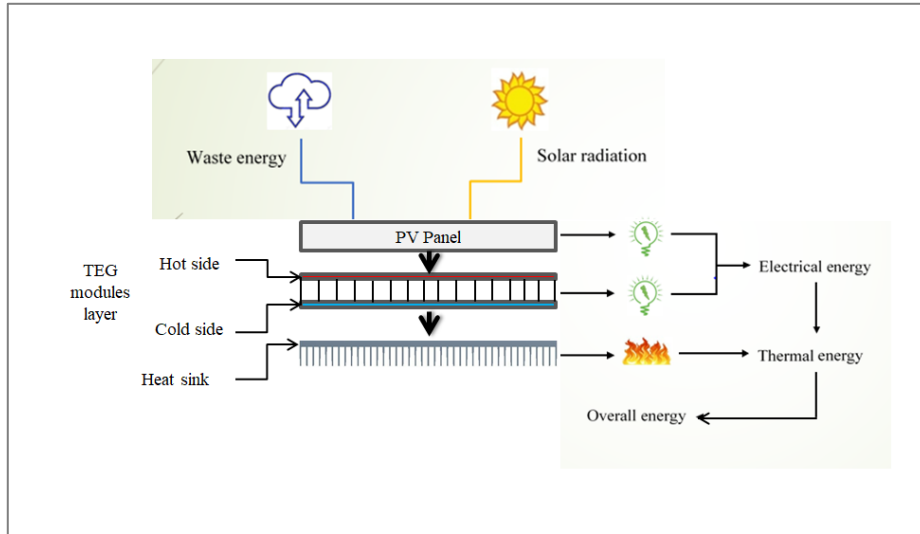


2.2. System Operation

When the solar panel is turned on and the sun's rays hit the top of the module, some of the energy is transformed into PV power, some of it is lost to the environment (through radiation and convection from the glass layer), and the rest is transferred to the TEG module via conduction heat transfer. Finally, the Seebeck effect predicts that some of the heat energy taken in by the TE module can be converted into electricity.

On the other hand, the heat sink draws most of the heat away from the TEG's cool side via a conduction transfer effect that travels along the fins. The energy flow of the hypothetical PV-TEG system is depicted in Figure 3.

Figure 3. Illustrates the energy pathway for the simulated PV-TEG system.



2.3. System Model

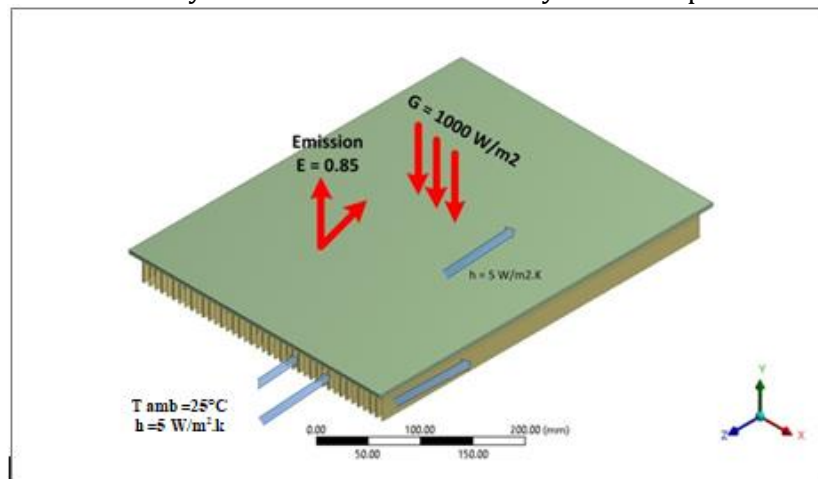
In this study, a hybrid system is more complicated than a conventional PV and PV/T system. For facilitations, the parameters adopted for the account are inserted in Table 2 and limitations of the PV-TEG system model are depicted in Figure (4). Following assumptions are accepted in numerical simulation and data reduction (Hashim 2015) and (Gu et al. 2019):

- The simulation is three-dimensional and uses a steady-state heat transfer mechanism. On the surface at the same height, the heat flux and temperature values are uniform and considered only in the direction of flow.
- Sides and backside heat losses are negligible.
- Properties of air and solid material are constant.
- There is no thermal gradient in the glue layers(thermal paste) because their thickness is very thin, and their thermal conductivity is high.
- Physical parameters and the materials properties in the TE module are maintained to be constant and independent of the temperature.
- The transmissivity of Encapsulant (EVA) that is used to be 100% in the systems, the thermal resistance between adjacent layers is very low and negligible.

Table 2. Parameters are used in calculations(Hashim 2015)

Parameter	Value (Unit)
τ_g	0.95
β_c	1
α_c	1
α_t	0.5
G	1000 (W/m ²)
ϵ	0.85
σ	$5.62 \cdot 10^{-8}$
α	$1.85 \cdot 10^4$ (VK ⁻¹)
β_0	0.0041 (K ⁻¹)
ρ	$1 \cdot 10^{-5}$ ($\Omega \cdot m$)

Figure 4. Boundary conditions of the PV-TEG system with passive cooling.

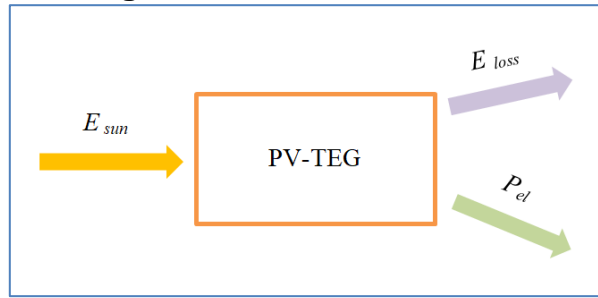


It should be noted that, Radiation is modeled as heat flux of 1000 W/m² projected on external surface of glazing glass layer. Heat loss through radiation (from cell to ambient) is a function of surface temperature of glass. emissivity ϵ is 0.85 and ambient temperature is 25 °C. The temperature of T_{sky} is considered as a T_{amb} (Hashim 2015). The wasted heat by free convection is modeled using stagnant air case (V_w) through heat transfer coefficient $h = 5$ W/m².K. Convection is applied at the upper, lower and side surfaces of the PV cell. The convective heat transfer coefficient (h) is estimated using the following correlations(Mohammad Sardarabadi 2016):

$$h = 5.7 + 3.8 V_w \quad (1)$$

where h and V_w represent the air velocity over the glass surface, sides, and fins of a heat sink, respectively. Further, the wind is indicated by the subscript w . Consider the complete PV-TEG installation as the control volume, then the energy balance for the system may be stated as shown in Figure (5).

Figure 5. PV-TEG control volume.



E_{sun} , E_{loss} , and P_{el} in Fig. 5 stand for solar input, losses, and produced electricity, respectively. E_{sun} , the solar radiation entering the PV alone, PV/T, and PV-TEG systems, may be determined by using the following formula. (Mohamed Selmi, Mohammed J. Al-Khawaja 2008):

$$E_{sun} = G \cdot A_{PV} \cdot \tau_g \cdot a_{cell} \quad (2)$$

where G represents the solar irradiance, A_{PV} is the solar panel's area, τ_g is the glass cover's transmissivity, and a_{cell} is the PV cell's absorptivity. In photovoltaic (PV), photovoltaic(PV/T), besides photovoltaic thermoelectric generator(PV-TEG) systems, the electrical output power of the PV panel ($P_{el, pv}$) can be computed as(Evans 1981):

$$P_{el, pv} = \eta_o \cdot [1 - 0.0041 \cdot (T_{cell} - 298.15)]. \tau_g \cdot G \cdot A_{PV} \quad (3)$$

with T_{cell} standing for the typical temperature of the PV cell. Furthermore, η_o reflects the assumed 8% PV module efficiency under standard test settings in this analysis.

In addition, output electrical power of TEG, ($P_{el, TEG}$) is defined in place of (D.M. Rowe, Ph.D. 2006):

$$P_{el, TEG} = \eta_{TEG} \cdot Q_{TEG} \quad (4)$$

Where, η_{TE} and Q_{TE} are the electrical efficiency of the TEG modules and heat transfer by conduction through TEG, respectively. Q_{TEG} and η_{TEG} are defined as (Hashim 2015):

$$Q_{TEG} = \frac{M \cdot K_{TEG} \cdot A_{TE} \cdot N}{L_{TE}} \cdot (T_H - T_C) \quad (5)$$

Where M is the number of TEG modules, the thermal conductivity of the TE is K_{TEG} , N is pair number of thermoelements, L_{TE} is length of thermoelements, and T_H and T_C are the hot and cold sides of TEG modules temperatures (Sark 2011):

$$\eta_{TEG} = \frac{T_H - T_C}{T_H} \cdot \frac{\sqrt{1 + ZT_m} - 1}{\sqrt{1 + ZT_m} + \frac{T_C}{T_H}} \quad (6)$$

Where Z is refigure of merit and equal to $Z = \frac{\alpha^2}{\rho K_{TEG}}$, and $T_m = \frac{T_H + T_C}{2}$ is the mean temperature across the TEG module after substituting value of Z and T_m in equation (6), The output power of the TEG is ($P_{el, TE}$) can be calculated by substituting equations (5) and (6) in the equations(4).

Furthermore, the total electrical power generated by the (PV-TEG) hybrid system (P_{el}) is calculated by (Kossyvakis, Voutsinas, and Hristoforou 2016):

$$P_{el} = P_{el,PV} + P_{el,TEG} \quad (7)$$

The overall electrical efficiency of hybrid system is defined as (Abdelhak Lekbir, Samir Hassani, Mohd Ruddin Ab Ghani, Chin Kim Gan, Saad Mekhilef 2018):

$$\eta_{el} = \frac{P_{el}}{G.A_{PV}} \quad (8)$$

In addition, experimental output electrical power of TEG, ($P_{el,TEG}$) is calculated by using following formula [11]:

$$P_{TEG} = V_{oc} * I \quad (9)$$

Where V_{oc} is the voltage of a thermoelectric generator and was given by:

$$V_{oc} = \alpha_{np} * \Delta T \frac{R_L}{R_{in} + R_L} \quad (10)$$

Where R_L is the load resistance, R_{in} is the internal resistance of TEG, $\Delta T = (T_h - T_c)$ is the temperature difference across the two junctions, and α_{np} is referred to as the Seebeck coefficient. The electric current (I) flowing through the thermoelectric generator was given by:

$$I = \frac{s}{(1+s)^2} \frac{(\alpha_{np} * \Delta T)^2}{R_{in}} \quad (11)$$

Where $s = R_L/R_{in}$ is the ratio of the load resistance to the device's internal resistance. The power output depends on the ratio s , and the maximum power output was obtained at the matched load (i.e., when $R_L = R_{in} = 2.05\Omega$)

So total output P_{TEG} of all thermoelectric modules ("J.Energy.2016.01.055." n.d.):

$$P_{TEG} = \frac{V_{oc}^2}{4R_{in} * M} \quad (12)$$

The improvement ratio and the deviation (difference) percentage are calculated as ([https:// www. calculator.academy](https://www.calculator.academy), 'improvement-percentage-calculator' n.d.):

$$\text{The improvement ratio} = \frac{\text{Final value} - \text{Starting value}}{\text{Starting value}} * 100\% \quad (13)$$

$$\text{The deviation (difference) percentage} = \frac{\text{Final value} - \text{Starting value}}{\text{Final value}} * 100\% \quad (14)$$

3. Numerical Simulation

To gain from the comparison, the commercial program ANSYS workbench (2019R3) was used to create and simulate a 3D model of PV, PV/T, and seven models of PV -TEG temperature profiles under boundary limited conditions. Computational models of comprehensive is Transient Thermal in ANSYS Workbench for passive cooling cases (PV, PV/T and 7 models of PV-TEG). Transient Thermal solver provides the ability of obtaining minimum, maximum and average temperatures versus time directly. The end time is 7200 s (2 hrs.) with time step of 60 s. This solver also contains the options to add convection and radiation conditions.

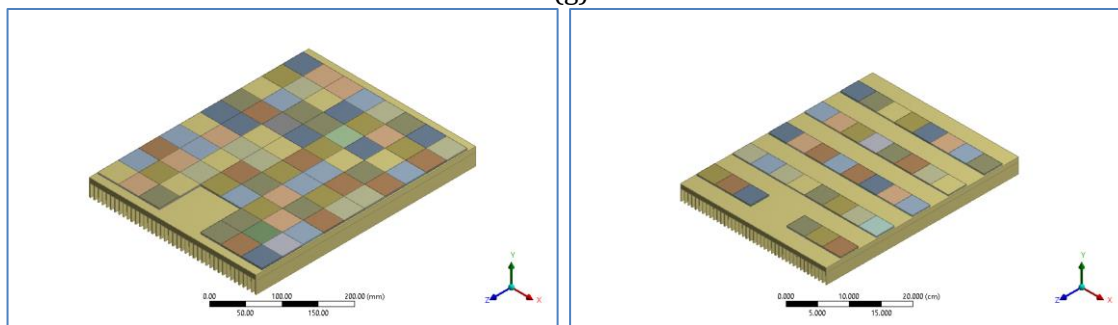
The simulated models of hybrid system that are analyzed and arranged as following:

- M1: The hybrid system (PV + 76 TEG modules full covered the backside of the PV module.
- M2: The hybrid system (PV + 38TEG modules are row arranged on the backside of the PV module.
- M3: The hybrid system (PV + 36 TEG modules are column arranged on the backside of the PV module.
- M4: hybrid system (PV+ 18TEG modules are matrix arranged on the backside of the PV module. Space between TEG item and another is 4 (cm).
- M5: The hybrid system (PV + 18 TEG modules are matrix arranged on the backside of the PV module. The space between TEG item and another is 5 (cm).
- M6: The hybrid system (PV + 11 TEG modules are matrix arranged on the backside of the PV module. The space between TEG item and another is 6 (cm).
- M7: The hybrid system (PV + 11 TEG modules are matrix arranged on the backside of the PV module. The space between TEG item and another is 7 (cm).

Figures (6) shows the 3D geometry of arrangement TEG modules with heat sink (passive cooling system) in the hybrid system models for M1:M7.

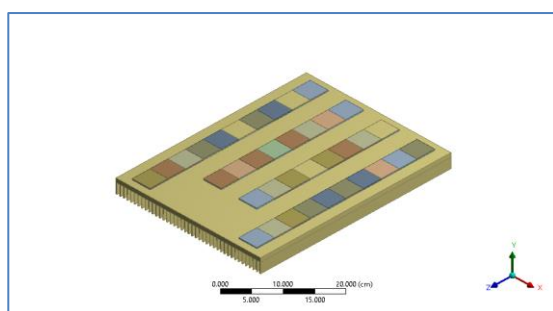
Figure (7)depicts a logic flow chart representing established computational models of PV-TE system.

Figure 6. the3D geometry of arrangement TEG modules with heat sink (passive cooling system) in the hybrid system models for (a)M1,(b)M2,(c)M3,(d)M4,(e)M5,(f)M6, and(g)M7

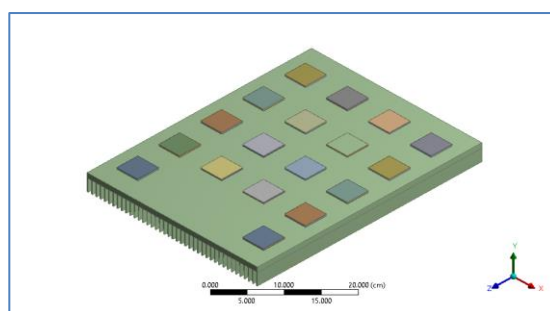


(a)M1 model

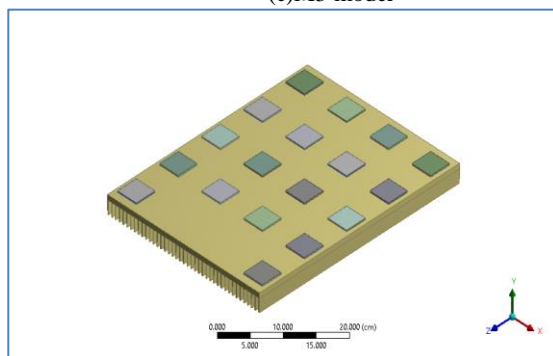
(b)M2 model



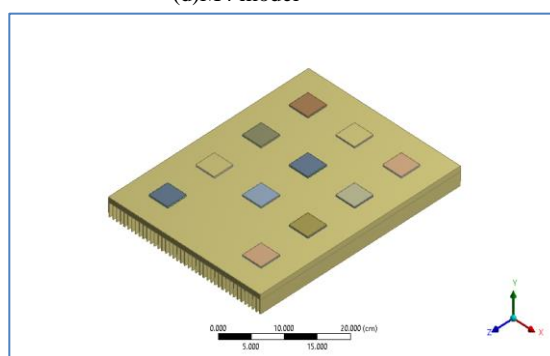
(c)M3 model



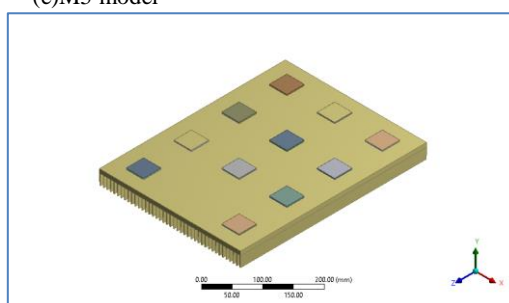
(d)M4 model



(e)M5 model

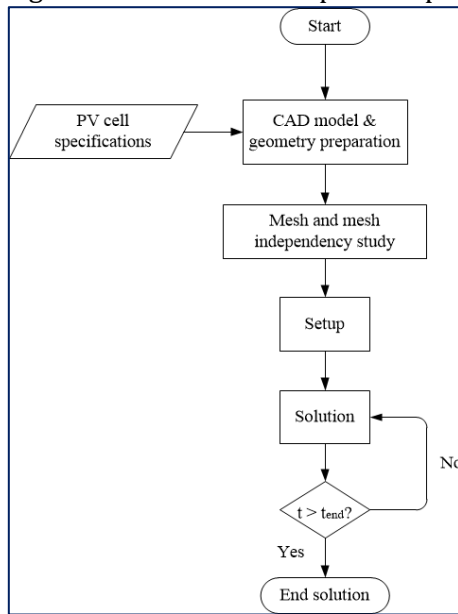


(f)M6 model



(g)M7 model

Figure 7. The logic flow chart of developed computational model.



The mesh analysis using these relations is presented in the following subsection.

4. Mesh Study

4.1. Mesh Independence Study

To get reliable, mesh-independent results at a reasonable computational cost, mesh -

Figure 8. Mesh independence study results

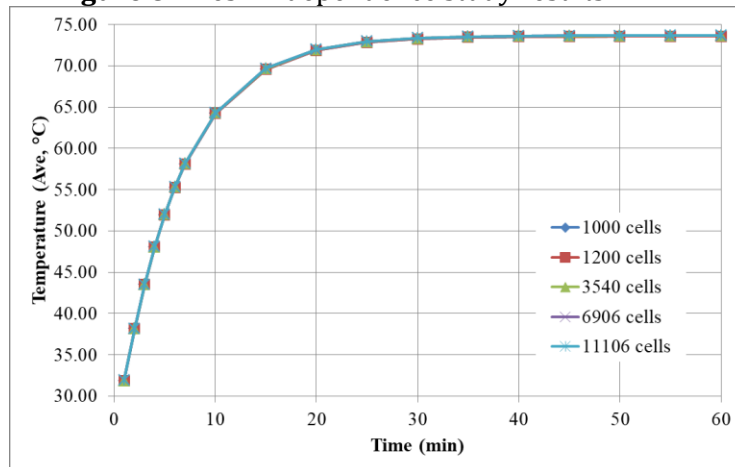
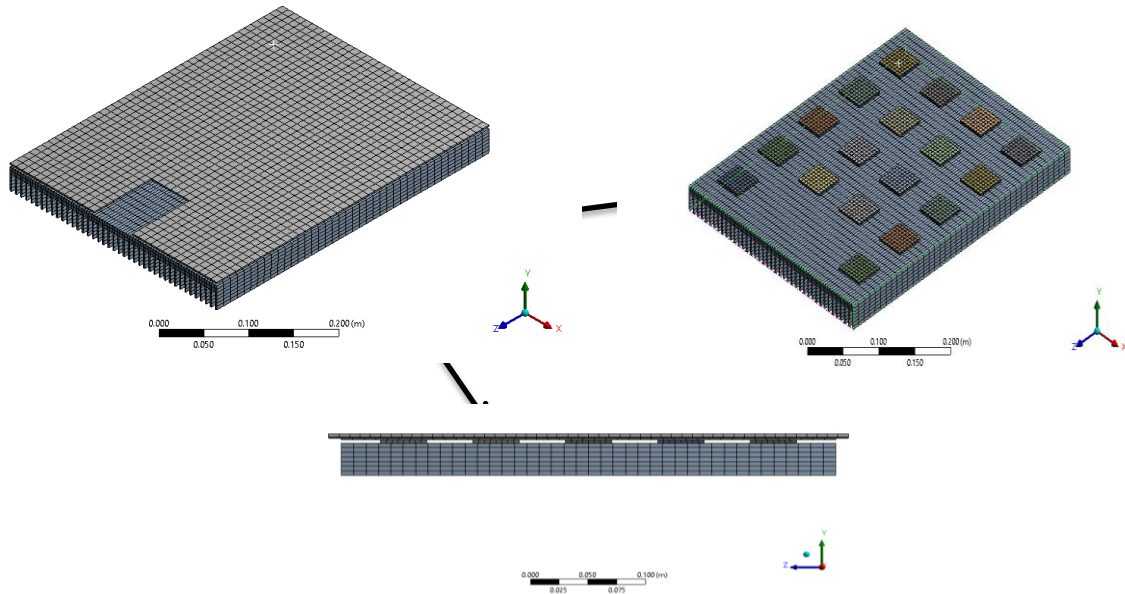


Figure 9. Mesh generated of M4 hybrid system



4.1.1. Mesh Quality Assessment

The produced mesh for PV-TE systems is checked for accuracy via two metrics—Orthogonal Quality(OQ) also skewness—to guarantee reliable simulation results (Ali Salari, Ali Parcheforosh, Ali Hakkaki-Fard 2020). Values suggested for OQ besides skewness measures are listed in Table (3).

The vast majority of the cells in this table have skewness and OQ values that fall within the high quality range. The lowest OQ value and highest skewness value are 0.9867 and 0.12001, respectively.

Table 3. Parameter ranges for orthogonal quality also skewness measures

Quality	OQ	Skewness
Excellent	1.00 - 0.95	0 - 0.25
Very good	0.95 - 0.70	0.25 - 0.50
Good	0.70 - 0.20	0.50 - 0.80
Acceptable	0.20 - 0.15	0.80 - 0.94

5. Experimental Work

To validate the performance of the optimum model of PV- TEG hybrid system , The experimental rig test stages were carried out under indoor exposure within the laboratory conditions in the Mechanical Department- College of Engineering at the Kerbala University. According to the results that will be displayed in section 5, the optimum model of hybrid system is M1 model. Figure (10) shows the schematic diagram of M1 model and measurement instrumentations. Photograph and experimental test rig of M1 model with PV/T system are displayed in Figure (11). In addition of the TEG modules arrangement and linking with heat sink are showed in Figure (12).

Figure 10: Schematic diagram of the M1 model of PV -TEG system.

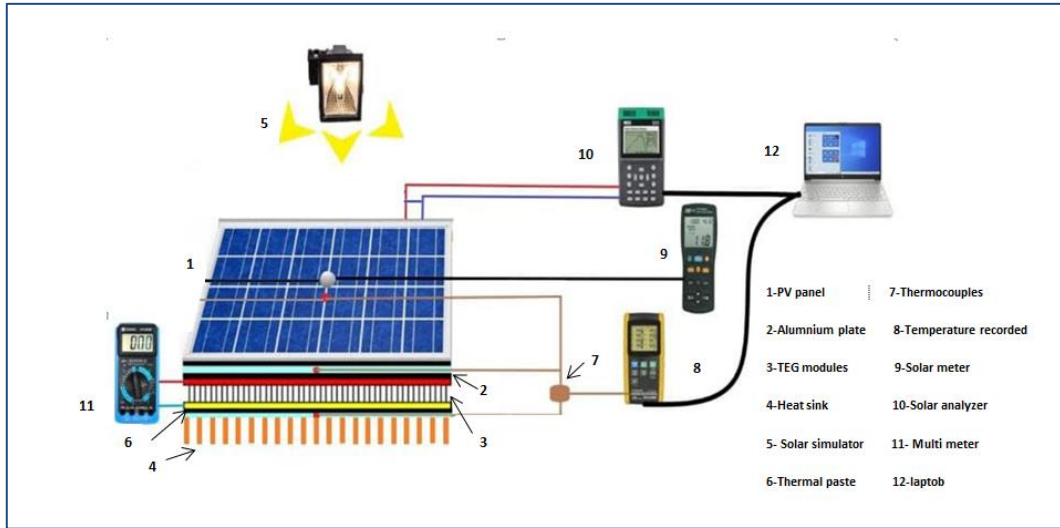


Figure 11: Photographs of experimental rig of M1model hybrid system , PV/T systems and PV panel

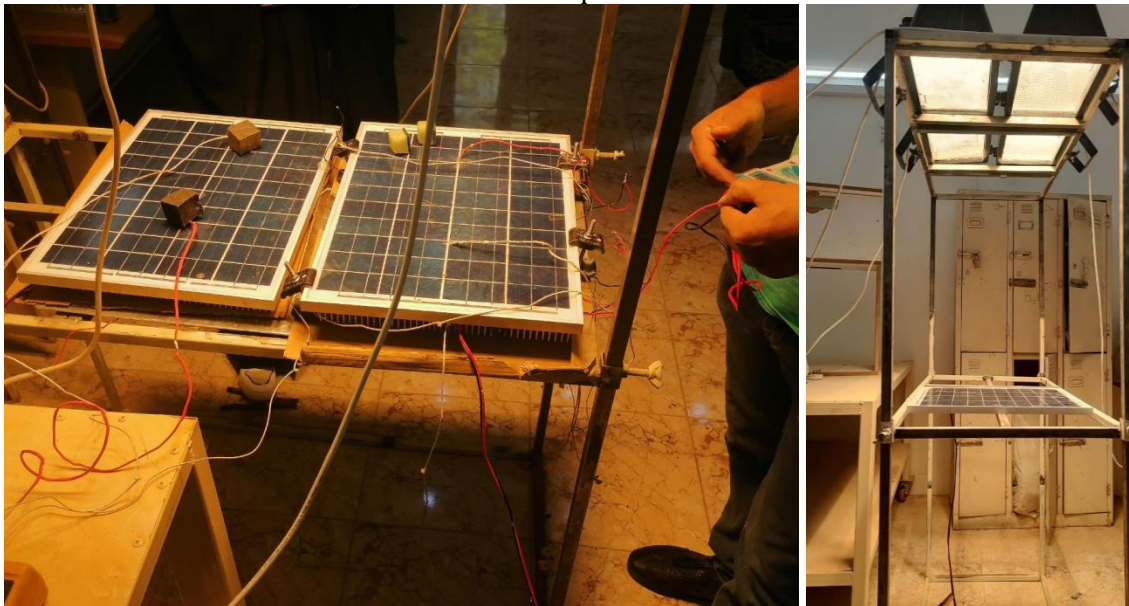


Figure 12: Actual photographs of experimental of TEG modules arrangement and linking with heat sink



6. Results and Discussion

6.1. Numerical Results

6.1.1. Temperature Distribution

After solution is converging, the temperature distribution on the surfaces of each layer in the all mentioned systems is calculated at each step of the solution technique, as shown in Figures (13) to (16). The average temperature on the glass layer in each of the tested systems is assumed toward be equal to PV surface temperature. Also, average temperature of both TEG sides, hot and cold, and other surfaces is calculated, as shown in Table (4).

Figure 13. Temperature distribution contour on the PV system surface

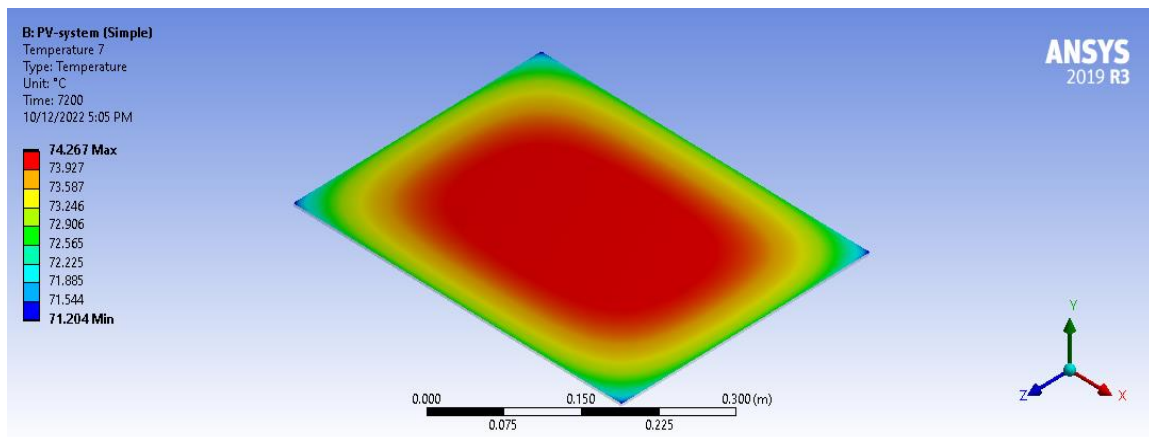


Figure 14. Temperature distribution contour on the PV surface in the PV/T system

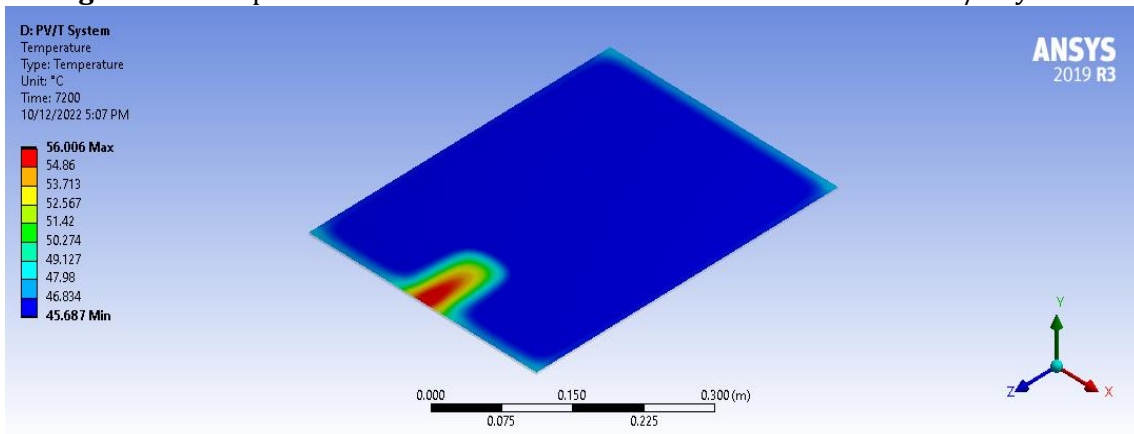
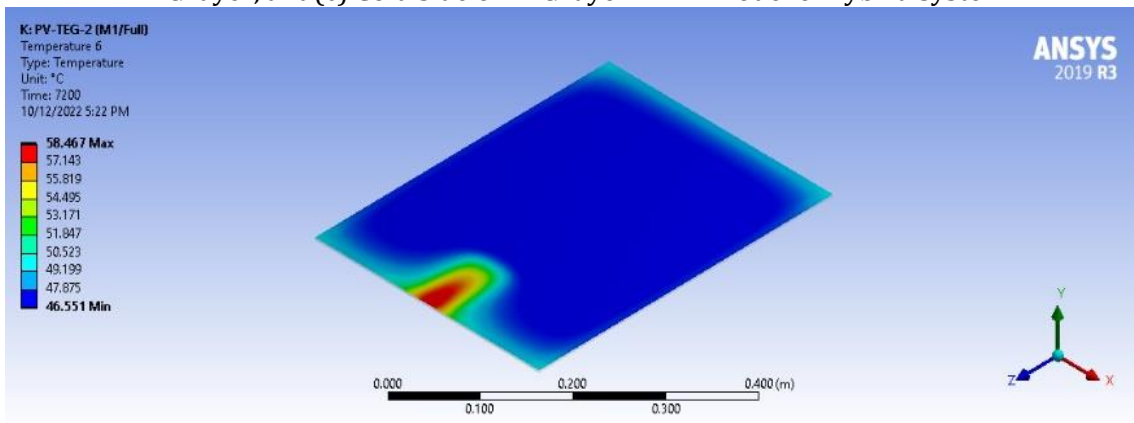
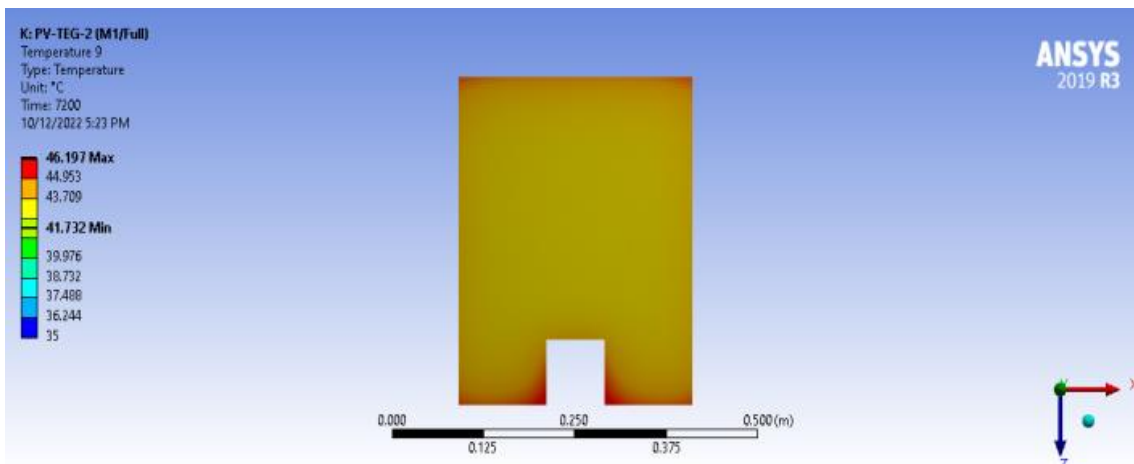


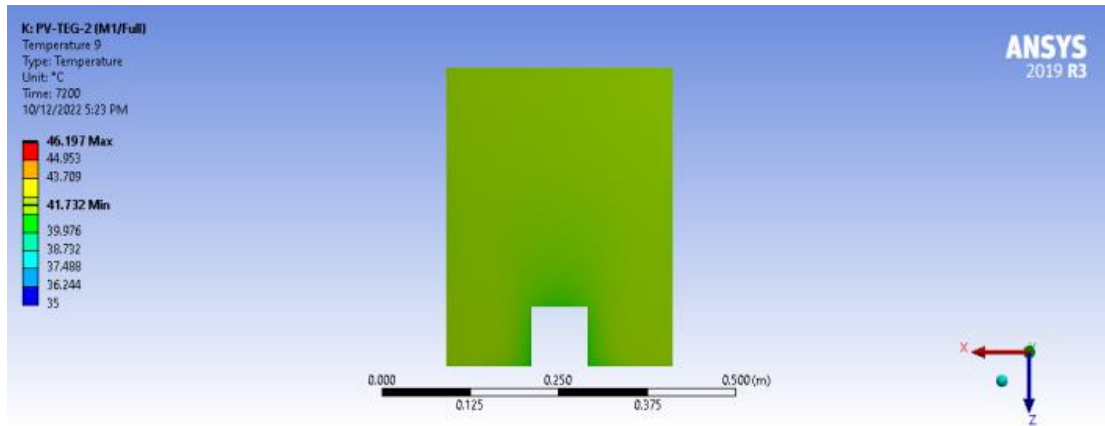
Figure 15. Temperature distribution on the; (a) Upper surface of PV layer, (b) Hot side of TEG layer, and (c) Cold side of TEG layer in M1 model of hybrid system.



(a) Upper surface of PV layer

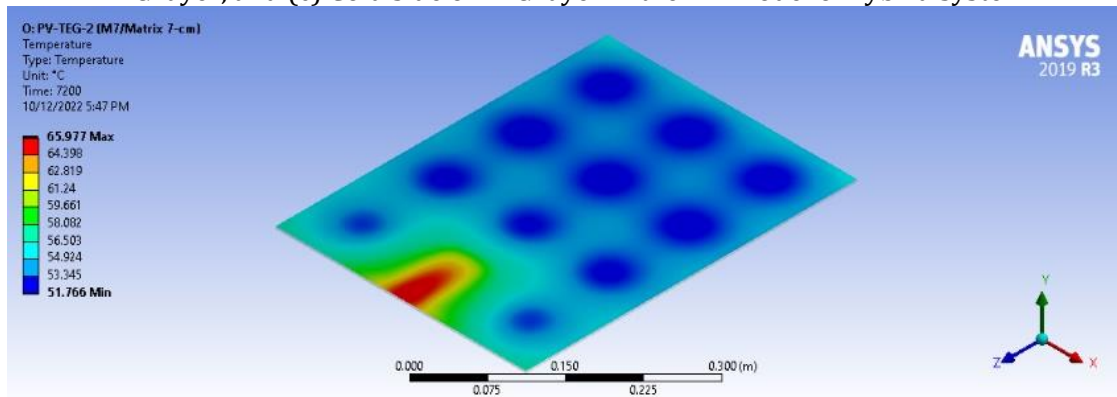


(b) Hot side of TEG layer

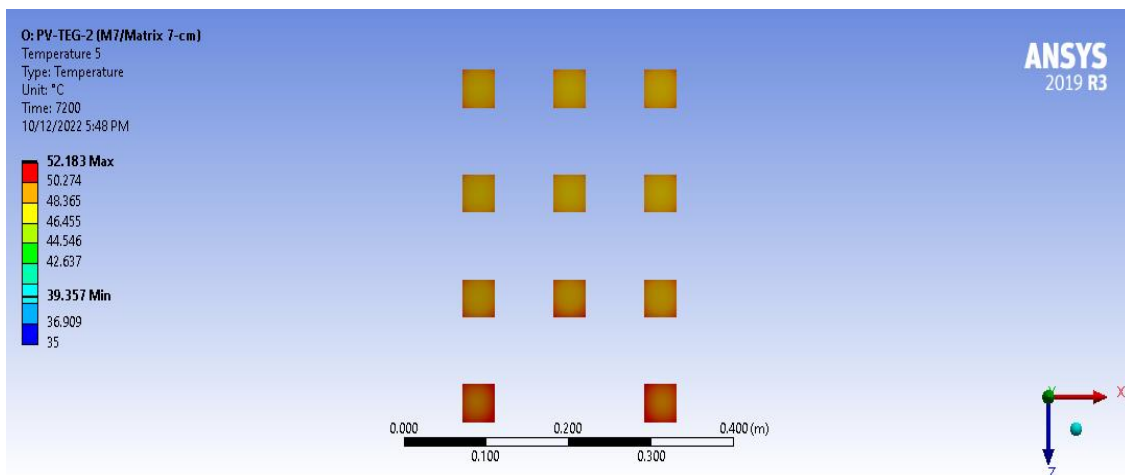


(c) Cold side of TEG layer

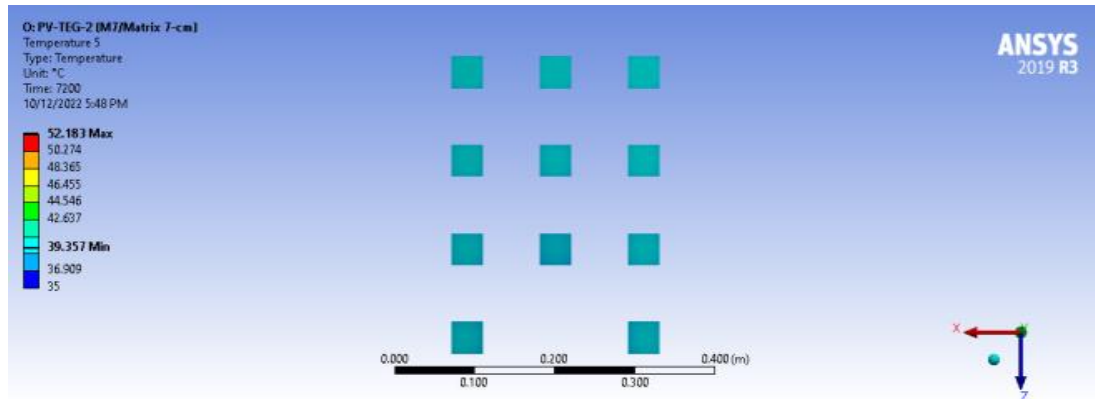
Figure 16. Temperature distribution on the; (a) Upper surface of PV layer, (b) Hot side of TEG layer, and (c) Cold side of TEG layer in the M7 model of hybrid system.



(a) Upper surface of PV layer



(b) Hot side of TEG layer



(c) Cold side of TEG layer

Table 4. Numerical results of temperature distribution for tested systems

SYSTEMS	T _{cell} (°C)	T _{hot} (°C)	T _{cold} (°C)	ΔT (°C)
M1	47.95	43	41.4	1.6
M2	48.9	44.18	41.05	3.18
M3	48.8	44.3	40.98	3.28
M4	51.5	46.35	40.16	6.19
M5	51.2	46.48	40.26	6.22
M6	54.4	48.8	39.3	9.47
M7	54.2	48.9	39.49	9.5
PV	73.3	-	-	-
PV/T	46.76	-	-	-

It can be seen that, the average temperature of PV module upper surface for PV panel is higher compared with other models of hybrid system and PV/T system due to the wasted heat from absorbed solar energy and lack of cooling device. In addition of , the average temperature of PV module upper surface that increases with decrease TEG items in the models of hybrid system. Because of thermoelectric modules effect that absorbs a thermal emission from the back of the PV panel, the average temperature of PV module upper surface decreases with TEG number increases. Also, it can be noticed that hot side temperature of TEG in each models is high depending on PV temperature. At same time, the cold side temperature of TEG is high due to low cooling effect of passive cooling system. Furthermore, the average temperature of PV module upper surface for PV/T system is about 46.76 and lower than that of PV panel and other models of hybrid system due to heat sink effect.

6.2. Optimum Model of Hybrid System

Dependent on the PV surface temperature profile, the solar radiation level, and the principle of data reduction by entering average temperature values of PV in system-governing equations in Section (2.3), the efficiency also output power of PV can be predicted in each the photovoltaic only, the PV/T system and M1, M2, M3, M4, M5, M6, and M7 hybrid system models as offered in Table(5). Figure (17) shows that the M1 model is the optimum model of hybrid system. At M1 model, the additional generated energy via TEG modules is higher than that of other models. In addition, this generated energy compensates for the power loss from PV panel

as result of PV temperature increase. Furthermore, M1 model performance is compared with that PV panel and PV/T system, as depict in Figure (18). The M1 model's electrical power production is clearly more than that of the PV alone also the PV/T systems through 16.3 percent in addition 1.7 percent, respectively.

Table 5. The output power and the overall electrical efficiency in the photovoltaic only, the PV/T system and M1, M2, M3, M4, M5, M6, and M7 hybrid system models

SYSTEMS	$P_{el,pv}$ (W)	$P_{el,TEG}$ (mW)	η_{pv} %	P_{el} (W)	η_{el} %
M1	10.427	160	7.17	10.587	6.92
M2	10.39	157.85	7.15	10.55	6.898
M3	10.38	157.8	7.14	10.54	6.889
M4	10.25	147.96	7.04	10.395	6.789
M5	10.24	147.9	7.056	10.38	6.8
M6	10.1	138.2	6.94	10.23	6.68
M7	10.08	138	6.95	10.22	6.69
PV panel	9.1	-	5.94	9.1	5.94
PV/T	10.45	-	6.83	10.45	6.83

Figure 17. The relationship of electrical output power for hybrid system models

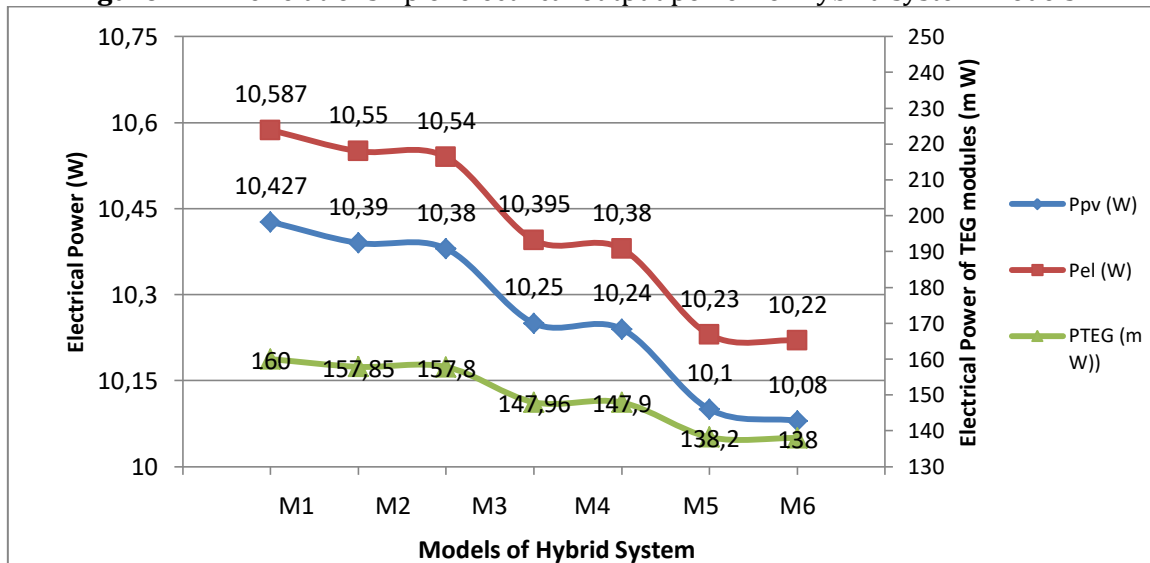
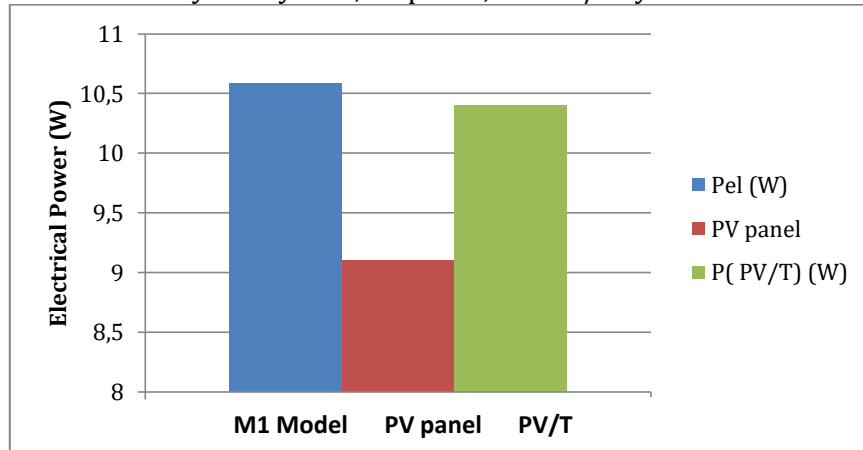


Figure 18. The comparison of electrical output power between the optimum model (M1) hybrid system, PV panel, and PV/T system



6.3. Experimental Results

The outcomes of the experiments included temperature measurements, electrical measurements, and calculations of performance based on the measurements, as shown below:

6.3.1. Temperature Measurements

The temperature measurements include the ambient temperature, front surface temperatures of PV cells, and inlet and outlet cooling water temperatures. As well as, the Aluminum plate temperature that is closed to the TEG hot side temperature (T_h) and the upper surface temperature of the heat sink that is assumed equal to the TEG cold side temperature (T_c) in the test systems as shown in Table (6). The results show that the average temperature of the PV module's front surface, is about 73 °C for the PV panel, 46.45 °C for the PV/T system, and 47.05°C for the M1 model PV-TEG hybrid. It also can be seen that (T_{sc}) in the PV panel due to the heat generated from absorbed solar energy and the lack of a cooling device. Furthermore, the T_{sc} is higher in M1model PV-TEG hybrid system compared to PV/T system because the presence of a layer of thermoelectric modules between the back surface of the PV module and the heat exchanger, that acts as a resistance and raises the temperature of the photovoltaic panels.

Table 6. The average temperature of the; Upper surface of PV layer, hot side and cold side of TEG layer, output power and the overall electrical efficiency in the photovoltaic only, the PV/T system and M1 hybrid system models

System	T_{sc} (°C)	T_h (°C)	T_c (°C)	P_m (W)	PTEG (mW)	P_{el} (W)	η_{el} (%)
PV panel	73			9.04	-	9.04	5.6
PV/T	46.45			10.4	-	10.4	6.78
M1 (PV-TEG)	47.05	42.4	40.9	10.35	59	10.41	6.8

6.3.2. Total Electrical Output Power

By connecting the PV module wires to the PROVA 200A Solar Analyzer, the electrical measurements are recorded, which include the maximum power point (MPP) features electrical power (P_m). Digital Multi meter Type TMT 4600 was also

used to record the total open voltage (V_{oc}) of the thermoelectric modules. The calculated results are shown in Table (6). The maximum electrical output of PV cells products of the current multiplied by the voltage at maximum power point which declines with rising temperature by (0.4–0.5) %. It can be seen that instantaneous maximum power (P_m) of the solar PV/T system is more than the power of the PV module under 1000 (W/m^2) the solar irradiance, due to the cooling the PV module keeps voltage of PV module from decrement. Therefore, this effect would raise the electrical power. On the other hand, the PV-TEG, outperformed all other test systems because of the extra power produced by the thermoelectric during the conversion of wasted heat into electricity which is calculated by using the equation (12). In a fixed-light scenario, the improvement ratio of output power of PV-TEG (M1) model is higher by 15.13 and 0.8 % than that of the traditional photovoltaic alone and the PV/T system, respectively.

6.4. Comparing of Numerical and Experimental Results

Numerical results, such as (T_{sc} and P_{el}) are validated by comparing them with experimental data by calculating the deviation (difference) percentage between both results according to equation (13). The difference percentage between numerical and experimental results of average temperature of the PV module top surface (T_{sc}) are (0.4 %, 0.7 %, and 1.87%) for the PV panel, PV/T system, and PV-TEG hybrid system, respectively as shown in figure (19). In addition, the difference percentage of the electrical output power (P_{el}) between numerical and experimental results are (0.6 %, 0.66 %, and 1.67 %) for the PV panel, PV/T system, and M1 model of PV-TEG hybrid system, respectively as shown in figure (20). It can be seen that the numerical results for all studied parameters show a good level of agreement with experimental results.

Figure 19. Numerical and experimental results of average front surface temperature of PV in the PV panel, PV/T system, and PV -TEG hybrid system

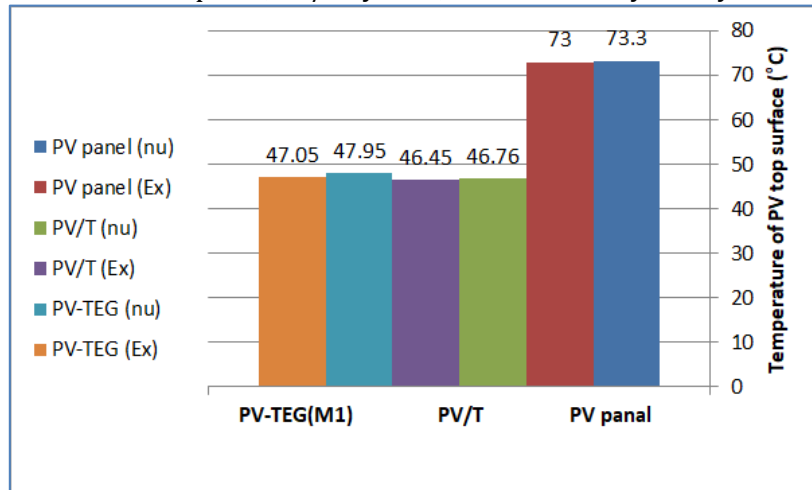
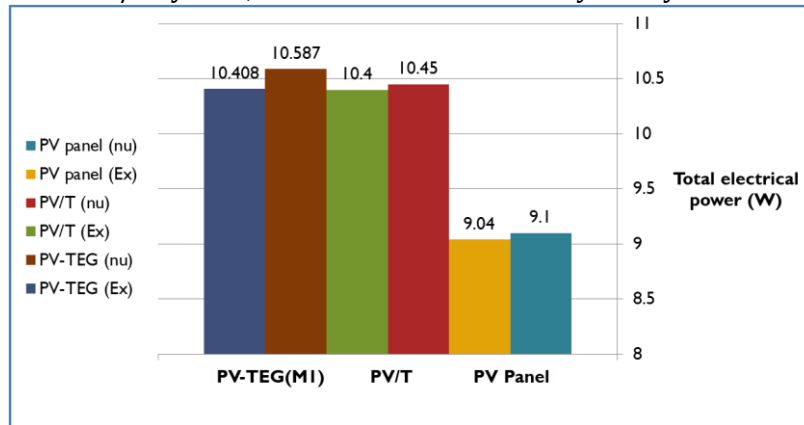


Figure 20. Numerical and experimental results of electrical output power of the PV panel, PV/T system, and M1 model PV -TEG hybrid system



7. Conclusion

In principle, a hybrid system consisting of photovoltaic (PV) solar cells and thermoelectric (TEG) devices may collect the solar cells' waste heat and turn it into usable electricity, lowering operating temperature of the solar cells, maintaining efficiency and their life time. In this study, numerical analysis of seven different models of hybrid systems (M1, M2, M3, M4, M5, M6, and M7) performance was performed via using commercial PV, different numbers of TEG modules, and heat sink under the same conditions. After comparing the theoretical results, the M1 model was the optimal design. When compared to the PV alone and PV/T systems, M1 model output power is higher by 16.3 and 1.79%, respectively. Experimentally, the enhancement ratio of P_{el} of the (M1) model is higher by 15.13 and 0.8 % compared with the photovoltaic panel and the PV/T system. The numerical results for all studied parameters show a good level of agreement with experimental results. Ultimately, the PV-TEG hybrid system's performance was less affected by the passive cooling system than that of the PV/T system.

References

- Abdelhak Lekbir, Samir Hassani, Mohd Ruddin Ab Ghani, Chin Kim Gan, Saad Mekhilef, R. Saidur. 2018. "Improved Energy Conversion Performance of a Novel Design of Concentrated Photovoltaic System Combined with Thermoelectric Generator with Advance Cooling System." 19–29.
- Adham Makki, Siddig Omer, Yuehong Su, Hisham Sabir. 2016. "Numerical Investigation of Heat Pipe-Based Photovoltaic–Thermoelectric Generator (HP-PV/TEG) Hybrid System Adham." 274–87.
- Ali Salari, Ali Parcheforosh, Ali Hakkaki-Fard, Ali Amadeh PII: 2020. "A Numerical Study on a Photovoltaic Thermal System Integrated with a Thermoelectric Generator Module." 13039.
- Anon. 2016. "Model for Geometry Optimisation of Thermoelectric Devices in a Hybrid PV/TE System." *Renewable Energy* 87:458–63. doi: 10.1016/j.renene.2015.10.029.
- Anon. n.d. "J.Energy.2016.01.055.Pdf."
- Babu, Challa, and P. Ponnambalam. 2017. "The Role of Thermoelectric Generators in the Hybrid PV/T Systems: A Review." *Energy Conversion and Management* 151:368–85.
- D.M. Rowe, Ph.D., D. S. 2006. *THERMOELECTRICS HANDBOOK*. edited by D. S. D.M. Rowe, Ph.D. Taylor & Francis Group.
- Darkwaa, J., J. Calautit, D. Du, G. Kokogianakis. 2019. "A Numerical and Experimental Analysis of an Integrated TEG-PCM Power Enhancement System for Photovoltaic Cells." 688–701.
- Dianhong Li, Yimin Xuan, Qiang Li, Hui Hong PII: 2017. "Exergy and Energy Analysis of Photovoltaic-Thermoelectric Hybrid Systems."
- Evans, D. L. 1981. "Simplified Method for Predicting Photovoltaic Array Output." *Solar Energy* 27(6):555–60.
- Gu, Wenbo, Tao Ma, Aotian Song, Meng Li, and Lu Shen. 2019. "Mathematical Modelling and Performance Evaluation of a Hybrid Photovoltaic-Thermoelectric System." *Energy Conversion and Management* 198(March):111800. doi: 10.1016/j.enconman.2019.111800.
- H. Hashim, J.J. Bompfrey, G. Min. 2016. "Model for Geometry Optimisation of Thermoelectric Devices in a Hybrid PV/TE System." 458–63.
- Han Xue, Zhao Guankun, Xu Chao †, Ju Xing, Du Xiaoze, Yang Yongping, and Key. 2017. "Parametric Analysis of a Hybrid Solar Concentrating Photovoltaic/Concentrating Solar Power (CPV/CSP) System Han." 520–33.
- Hashim, Hasan Talib. 2015. "Full-Spectrum Solar Energy Harvesting Using Nanotechnology- Enabled Photovoltaic / Thermoelectric Hybrid System." (September):1–184.

- [https:// www. calculator.academy](https://www.calculator.academy), ‘improvement-percentage-calculator,’ 2022. n.d. “No Title.”
- Kossyvakis, D. N., G. D. Voutsinas, and E. V. Hristoforou. 2016. “Experimental Analysis and Performance Evaluation of a Tandem Photovoltaic-Thermoelectric Hybrid System.” *Energy Conversion and Management* 117:490–500.
- Krishnadass Karthick, Suresha, Mohammed Muaaz M.D. Hussain, Hafiz Muhammad Ali, C. S. Sujith Kumar. 2019. “Evaluation of Solar Thermal System Configurations for Thermoelectric Generator Applications: A Critical Review.” 111–42.
- M. Hajji, H. Labrim, M. Benaissa, A. Laazizi, H. Ez-Zahraouy, E. Ntsoenzok, J. Meot, A. Benyoussef. 2017. “Photovoltaic and Thermoelectric Indirect Coupling for Maximum Solar Energy Exploitation.” 184–91.
- M W Aljibory, H. T. Hashim and W. N. Abbas. 2021. “A Review of Solar Energy Harvesting Utilising a Photovoltaic–Thermoelectric Integrated Hybrid System.” 012115.
- Mahmoudinezhad, S., A. Rezaia, D. T. Cotfas, P. A. Cotfas, and L. A. Rosendahl. 2018. “Experimental and Numerical Investigation of Hybrid Concentrated Photovoltaic – Thermoelectric Module under Low Solar Concentration.” *Energy* 159:1123–31. doi: 10.1016/j.energy.2018.06.181.
- Mohamed Selmi, Mohammed J. Al-Khawaja, Abdulhamid Marafi. 2008. “Validation of CFD Simulation for Flat Plate Solar Energy Collector.” 383–87.
- Mohammad Sardarabadi, Mohammad Passandideh-Fard. 2016. “Experimental and Numerical Study of Metal-Oxides/Water Nanofluids as Coolant in Photovoltaic Thermal Systems (PVT).” 533–42.
- Mohsenzadeh, Milad, M. B. Shafii, and H. Jafari mosleh. 2017. “A Novel Concentrating Photovoltaic/Thermal Solar System Combined with Thermoelectric Module in an Integrated Design.” *Renewable Energy* 113:822–34.
- Riahia, Afifa, Abdessalem Ben Haj Ali, Abdelhamid Fadhel, Amenallah Guizani, Moncef Balghouthi. 2020. “Performance Investigation of a Concentrating Photovoltaic Thermal Hybrid Solar System Combined with Thermoelectric Generators.” 112377.
- Samson Shittu, Guiqiang Li, Yousef Golizadeh Akhlaghi, Xiaoli Ma, Xudong Zhao, Emmanuel Ayodele. 2019. “Advancements in Thermoelectric Generators for Enhanced Hybrid Photovoltaic System Performance.” 24–54.
- Sark, W. G. J. H. M. va. 2011. “Feasibility of Photovoltaic - Thermoelectric Hybrid Modules.” *Applied Energy* 88(8):2785–90.
- Yin, Ershuai, Qiang Li, and Yimin Xuan. 2017. “Thermal Resistance Analysis and Optimization of Photovoltaic-Thermoelectric Hybrid System.” *Energy Conversion and Management* 143:188–202.
- [https:// www. calculator.academy](https://www.calculator.academy), ‘improvement-percentage-calculator,’ 2022

© Copyright of Journal of Current Research on Engineering, Science and Technology (JoCREST) is the property of Strategic Research Academy and its content may not be copied or emailed to multiple sites or posted to a listserv without the copyright holder's express written permission. However, users may print, download, or email articles for individual use.